Jour. of the KGS, Vol. 23, No. 3. March 2007, pp. 111~121

Reliability Analysis of Seismically Induced Slope Deformations

신뢰성 기법을 이용한 지진으로 인한 사면 변위해석

Kim, Jin-Man[1] 김 진 만

요 지

지진하중의 불확실성을 평가할 수 있는 신뢰성기반 해석기법을 제시한다. 이 기법은 종래의 한계평형법과 뉴막-형식의 변형량 계산기법에 확률개념을 도입하였으며 피해 위험성을 몬테칼로 시뮬레이션 해석기법으로 계산한다. 지진파를 작성하고 이들을 사면 내진 해석에 사용하고자 확률변수 프로세스와 RMS 재해 기법을 도입하였다. 지반성질의 변동성과 통계오차도 고려하였다. 신뢰성 해석 결과 지진활동이 활발한 지역에서는, 계산된 사면파괴 위험성과 과도한 영구변형의 관점에서 비교할 때 지진재해 평가가 더 중요한 사항이며, 재료성질의 묘사방법의 차이는 상대적으로 영향이 적다는 사실이 밝혀졌다. 이 결과는 원형 및 비원형 형태의 활동면 파괴에 모두 해당된다.

Abstract

The paper presents a reliability-based method that can capture the impact of uncertainty of seismic loadings. The proposed method incorporates probabilistic concepts into the classical limit equilibrium and the Newmark-type deformation techniques. The risk of damage is then computed by Monte Carlo simulation. Random process and RMS hazard method are introduced to produce seismic motions and also to use them in the seismic slope analyses. The geotechnical variability and sampling errors are also considered. The results of reliability analyses indicate that in a highly seismically active region, characterization of earthquake hazard is the more critical factor, and characterization of soil properties has a relatively small effect on the computed risk of slope failure and excessive slope deformations. The results can be applicable to both circular and non-circular slip surface failure modes.

Keywords : Artificial motion, Monte carlo simulation, Random process, Reliability, Seismic slope stability

1. Introduction

An important step in the slope stability analysis is to identify uncertainties of key design parameter and their statistics. The variability of the various parameters such as material properties, fluctuations of the loads, and the uncertainties of the geometry all contribute to the difficulty of evaluating how the slope actually behaves regardless of the computed factor of safety. In spite of extensive effort, there has not been much consensus on how to model these uncertainties systematically, leaving them mostly up to the rather subjective judgments of individual engineers. In the past, there have been numerous studies of the various sources of uncertainty and their impact on the risk of damage of slopes subjected to seismic loading. Most approaches, however, have focused either on material uncertainty or on uncertainty of seismic loading (e.g., Pal et al. 1991; Yegian et al. 1991) partly because of computational convenience, and partly due to the practical difficulty in modeling both material and seismic

1 Member, Assistant Prof., Dept. of Civil Engrg., Pusan National Univ., jmkim@pusan.ac.kr

hazard uncertainties.

Kim (2003) reported the importance of geotechnical variability in the analysis of earthquake-induced slope deformations. This paper reports follow-up analytical and numerical studies that investigated the influence of inherent variability and uncertainty of seismic loading in the analysis of seismic slope stability. Kim (2003) described some of the findings from that study and this paper reports all the remaining findings in details. In this paper, the author presents a reliability-based method that can capture the impact of uncertainty of key material properties and seismic loading in the assessment of seismic slope stability. The uncertainty of seismic loading is approached by generating a large series of hazard-compatible artificial motions, and by using them in subsequent response analyses. The geotechnical variability and sampling errors are also taken into consideration. This approach incorporates probabilistic concepts into the classical limit equilibrium and the Newmark-type deformation techniques. The authors adopt the so-called decoupled approach, where seismic response and deformation analyses are carried out separately, mainly because of its computational efficiency. The risk of damage is then computed by Monte Carlo simulation. Finally, the overall impact of uncertainties and their relative significance on seismic stability of slopes will be judged.

2. Generation of Hazard-Compatible Ground Motions

Due to the random nature of earthquake motions, the definition of the input excitation is one of the major uncertainties in the seismic response analysis. The stochastic representation of the earthquake motion hazard provides, at least theoretically, a systematic way of representing the infinite number of possible scenarios, which correspond to a certain level of hazard.

A series of sinusoids can be used to express a periodic function. With a zero-mean process, it can be represented as:

$$X(t) = \sum_{i=1}^{n} A_i \sin(\omega_i t + \theta_i) \tag{1}$$

where A_i is the Fourier amplitude, ω_i is the circular frequency, and θ_i is the phase angle of the i^{th} contributing sinusoid. By fixing an array of amplitudes and randomly generating different arrays of phase angles, we can produce different motions with the same general appearance but different details (Gasparini and Vanmarcke 1976). For a stationary random process, the Fourier amplitude A_i is related to the (one-sided) power spectral density function (PSD) $G(\omega)$ as:

$$\tfrac{1}{2} A_i^2 = G(\omega_i)\Delta\omega \tag{2}$$

The study adopts the following widely quoted form for the power spectral density function (PSD) that is based on Kanai (1957) and Tajimi (1960)'s studies.

$$G(\omega) = G_0 \frac{1 + 4\zeta_g^2(\omega/\omega_g)^2}{\left[1-(\omega/\omega_g)^2\right]^2 + 4\zeta_g^2(\omega/\omega_g)^2} \tag{3}$$

where $G(\omega)$ is the energy content at frequency ω, G_0 is some measure of shaking intensity, and ζ_g and ω_g are the parameters termed as "ground damping coefficient and frequency". Each different array of phase angles can be modeled by statistically independent random phase angles θ_i, which are uniformly distributed between 0 and 2π. Equation 1 then becomes (Rice 1954):

$$X(t) = \sum_{i=1}^{n} \sqrt{2G(\omega_i)\Delta\omega}\, \sin(\omega_i t + \theta_i) \tag{4}$$

As the number n of sinusoidal motions becomes large, the distribution of the process $X(t)$ approaches Gaussian distribution by virtue of the central limit theorem, as long as A_i is of similar magnitude (Yang 1973). Sample stationary earthquake motion (based on Equation 4) can then be obtained as shown in Figure 1.

The transient character of the intensity content of the earthquake motion can be added by multiplying the stationary motion by a deterministic modulating (envelope) function $m(t)$. The non-stationary motion $Y(t)$ then becomes

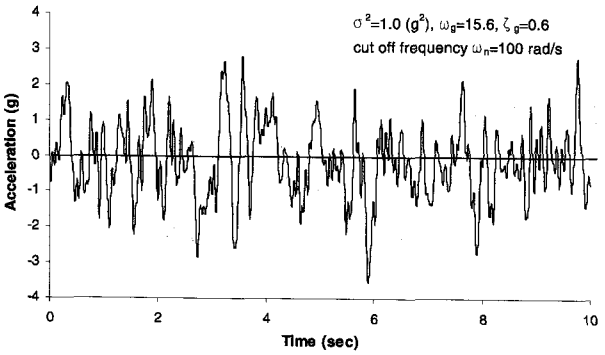

Fig. 1. Sample Stationary Artificial Earthquake Ground Motion for Rock Sites Based on the Frequency Parameters for Firm Soil Proposed by Kanai (1957)

$$Y(t) = m(t)X(t) = m(t)\sum_{j=1}^{n}\sqrt{2G(\omega_j)\Delta\omega}\,\sin(\omega_j t + \theta_j) \quad (5)$$

Various modulating functions have been used to incorporate non-stationary aspect of the earthquake ground motions. The most common forms of the modulating function are "Rectangular", "Exponential", "Trapezoidal", and their combination imitates initial build-up followed by a strong-motion part and then a die-down segment of typical recorded ground motions. In their liquefaction-related analytical approaches, Wang and Kavazanjian (1987) proposed a trigonometric modulating function that has two model parameters to define the shape of the modulating function as:

$$m(t) = \sin^{\alpha}\left(\pi(t/t_d)^{\beta}\right) \quad (6)$$

where α and β are two parameters to determine the shape of the modulating function and t_d is the duration of motion. The function is in a normalized form for both intensity and duration such as:

$$0 \le m(t) \le 1 \quad \text{and} \quad 0 \le t/t_d \le 1 \quad (7)$$

Unlike the conventional models, this model provides a convenient way in developing the statistics of shape parameters since it is in a normalized form and can thus be used independent of the intensity and the duration of the ground motion. For this reason, the model is adopted in our study. Wang and Kavazanjian (1987) also developed the statistics of the model parameters α and β based on their study of 122 Northern California strong ground motions.

The normalized PSD is obtained by dividing the PSD by the variance as:

$$G^*(\omega) = \frac{1}{\sigma^2}G(\omega) \quad (8)$$

When the stationary process $X^*(t)$ is a normalized process with unit variance and PSD function $G^*(\omega)$, Equation 5 (non-stationary ground motion) can be rewritten in terms of the normalized PSD function and modulating function $m(t)$ as:

$$Y(t) = m(t)X^*(t) = m(t)\sum_{i=1}^{n}\sqrt{2G^*(\omega_i)\Delta\omega}\,\sin(\omega_i t + \theta_i) \quad (9)$$

2.1 Intensity

Traditionally, most seismic hazard analyses use either maximum values of ground motion or a response spectrum to characterize the intensity of ground shaking (e.g., Housner 1952, Idriss 1991, Abrahamson and Silva 1996, 1997). However, using a maximum value to characterize the intensity of shaking is often inadequate, especially when dealing with structures whose response depends on total seismic energy rather than peak values of ground shaking. One of the energy-based parameters is the RMS (Root Mean Square) acceleration, which is defined as (Housner 1975):

$$RMS_a = \left[\frac{1}{T_d}\int_{t_0}^{t_0+T_d} a^2(\tau)d\tau\right]^{1/2} \quad (10)$$

where $a(t)$ is an acceleration time history, t_0 is a initial time of interest, T_d is duration of the strong ground shaking. Similarly, temporal RMS can be defined by replacing T_d with a small time interval Δt as:

$$RMS_a(t) = \left[\frac{1}{\Delta t}\int_{t}^{t+\Delta t} a^2(\tau)\,d\tau\right]^{1/2} \quad for\ \Delta t \to 0 \quad (11)$$

It is fairly straightforward to relate time-variant *RMS* to the deterministic modulating function $m(t)$ for the case

when $X^*(t)$ is a normalized process as follows:

$$RMS_Y^2(t) = E\left[Y^2(t)\right] = m^2(t)E\left[X^{*2}(t)\right] = m^2(t) \quad (12)$$

The time-variant *RMS* of the motion $Y(t)$ is thus identical to the modulating function $m(t)$ in case of the normalized process.

2.2 Frequency Content

There are different methods for characterizing the temporal variation of the spectral content of earthquake motion. A simple, yet efficient, approach is to divide the ground motion into several sections small enough so that stationarity of the frequency content within each section can be assumed without much error (Saragoni and Hart 1974). The proposal by Saragoni and Hart (1974) is based on dividing the motion into three sections of equal time interval as:

$$Y(t) = m(t)\sum_{j=1}^{3}\left(X_j^*(t_j)\right)$$

$$= m(t)\sum_{j=1}^{3}\left[\sum_{i=1}^{n}\sqrt{2G_j^*(\omega_i)\Delta\omega}\sin(\omega_i t_j + \theta_i)\right], \qquad t = \sum_{j=1}^{3} t_j \quad (13)$$

Once the number of sections is determined, the frequency and damping parameters of Kanai-Tajimi PSD need to be estimated for each section. Based on the approach by Saragoni and Hart (1974), Wang and Kavazanjian (1987) analyzed 80 out of the same set of 122 earthquake records, which were used to estimate the modulating function parameters, and proposed the statistics (i.e., mean and standard deviation) of the parameter ω_g and ζ_g. Tung et al. (1992) updated the statistics of modulating and PSD function parameters by including an additional set of 36 earthquake records from the 1989 Loma Prieta earthquake. These values are used in our analyses. Figure 2 shows a sample of non-stationary ground motion based on these statistics.

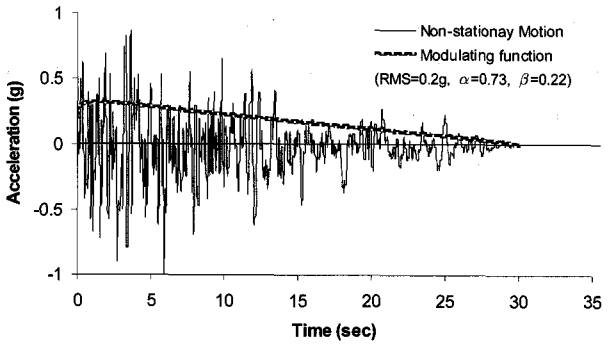

Fig. 2. Sample Time History of Non-Stationary Ground Motion (*RMS*=0.2 g, α=0.73, β=0.22, t_d=30 sec)

2.3 Duration

There are different definitions of duration including bracketed duration (Bolt 1969) and Arias duration (Trifunac and Brady 1975). 5-95% Arias duration (often called significant duration) is adapted in this study because it provides clear relationship to RMS hazard. The significant duration is nothing but the duration of the 5-95% RMS acceleration. Predictive relationships that relate the mean of 5-95% Arias duration with respect to the distance and moment magnitude (Abrahamson and Silva 1996) are used in this study.

3. Limit State Function and Monte Carlo Simulation

The performance of a structure can be described by a limit state function $g(\mathbf{x})$ such that failure is defined whenever the condition of $g(\mathbf{x}) \leq 0$ is satisfied, where $\mathbf{x}$ is the vector of model variables. The probability of failure is then given by:

$$p_f = P(g(\mathbf{x}) \leq 0) = \int_{g(\mathbf{x})\leq 0} f(\mathbf{x})\, d\mathbf{x} \quad (14)$$

where $f(\mathbf{x})$ is the joint probability density function (PDF) of $\mathbf{x}$. For deformation-based slope stability under static or seismic loadings, the limit state function can be formulated as:

$$g(\mathbf{x}) = D_a(\mathbf{x}) - D_p(\mathbf{x}) \quad (15)$$

where $D_a(\mathbf{x})$ and $D_p(\mathbf{x})$ denote the allowable and incurred deformations respectively. Particularly, the deformation-based limit-state function of a slope subject to seismic loadings can be obtained through ground response and slope

deformation analyses as shown in Figure 3.

Once the limit state function $g(\mathbf{x})$ and the distribution $f(\mathbf{x})$ are selected, the probability of failure p_f can be estimated by computing the volume of the joint distribution $f(\mathbf{x})$ within the failure domain defined by $g(\mathbf{x}) \leq 0$.

Classic Monte Carlo simulation involves the computation of deterministic solutions for a sufficient number of systematically generated realizations out of all possible scenarios. The resulting set of solutions is statistically analyzed to estimate means, variances, other higher moments, and possibly probability density functions. Recent advances in implementing methodologies, software, fast computing environments, and the use of optimization techniques (e.g., Rubinstein 1986) have made the Monte Carlo simulation one of the widely used practical tools in probabilistic analyses.

The numerical implementation and data flow of the proposed approach are illustrated in Figure 3. The author uses the so-called decoupled approach, in which seismic response and deformation analyses are carried out separately, mainly because of its computational efficiency. The analogy of a block resting on an inclined plane (so-called Newmark's method, Newmark 1965) is used for estimating the permanent displacement of the sliding mass due to earthquake shaking. The computation of yield acceleration is performed with newly developed expressions (Kim and Sitar 2004), which enable the calculation of the yield acceleration directly without iterations.

Probability computations (Equations 14) were carried out with the aid of CALREL, a general-purpose structural reliability analysis program developed by Liu et al. (1989). The program requires the definition of limit-state functions through user-defined subroutines. These user subroutines are written by the author in such a way that once statistics of seismic hazard, soil properties and geometry of the problem are provided, the program performs all sequential computations from the motion generation to deformation estimation without any interruption.

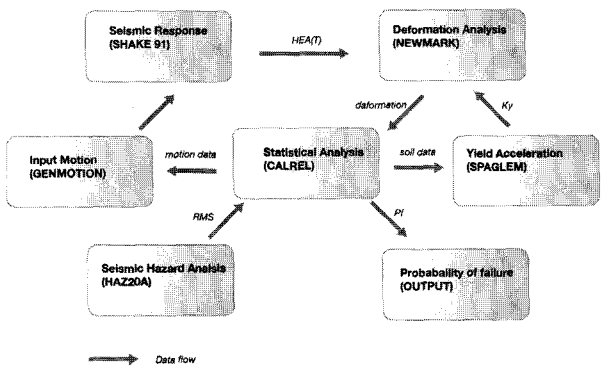

Fig. 3. Numerical Implementation and Data Flow of Probabilistic Seismic Slope Deformation Analysis

4. Illustrative Examples

The applicability of developed reliability-based methods is examined, starting from the analysis of seismically induced deformations of an idealized waste fill and ending with comparing the results with those of the seismic stability assessment of a homogeneous slope with a circular slip surface. Various levels of available information are examined in terms of their impact on the computed risk of slope failure.

4.1 Landfill (Non-Circular) Slope Stability

The author considers a problem where we are interested in evaluating the risk of failure of a solid-waste landfill slope along a gently sloping potential slip surface as shown in Figure 4. The geometry of the example landfill slope is very close to that of one of the failed landfill sections at Kettleman Landfill, reported by several researchers (e.g., Seed et al. 1990) and also similar to the damaged slope of Chiquita Canyon Landfills (e.g., Augello et al. 1995).

The key design parameters for both deterministic and probabilistic assessments of the landfill slope stability are given in Table 1. Sliding is assumed to occur only along the liner system underlying the waste-fill, since the foundation soil and waste-fill are judged to be much

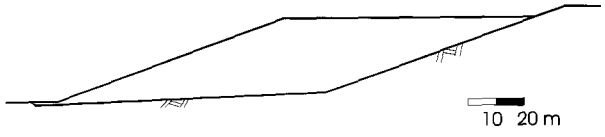

Fig. 4. Geometry of the Landfill Lying on the Gently Sloping Potential Slip Surface

Table 1. Key design material parameters

Parameter	Distribution	Mean	c.o.v.	No. of Tests	δ_x	δ_y
$\tan(\phi')$	lognormal	0.268	0.14	10	3 m	3 m
γ	deterministic	12 kN/m^3		10		

stronger than the liner interface (i.e., Kim et al. 2005). Accordingly, only the shear-strength properties of the liner interface, and the average density of the waste-fill deposit and soil cover overlying the lining system need to be considered. Expressions for characterization of material properties developed to incorporate sampling errors, spatial variation that were described in details by Kim (2003) are used, but are not repeatedly described here. The potential sliding mass is divided into 40 slices and Spencer method of analysis (as a subroutine of CALREL) is used to evaluate the limiting equilibrium. Figure 5 shows two different samples of generated friction coefficients over the 40 slices of the slip surface. It is worthy to note that sampling errors have the effect of shifting the trends of the generated soil properties from the sample mean.

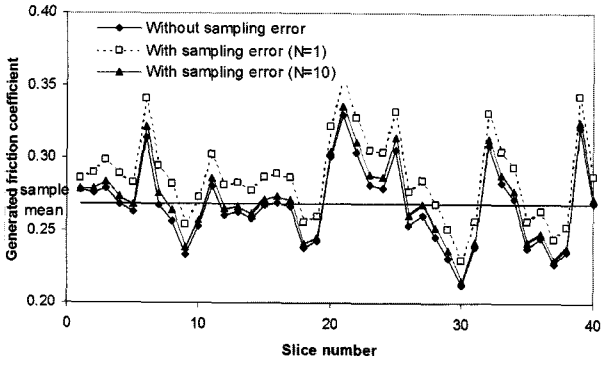

(a) with Trend Higher than the Sample Mean

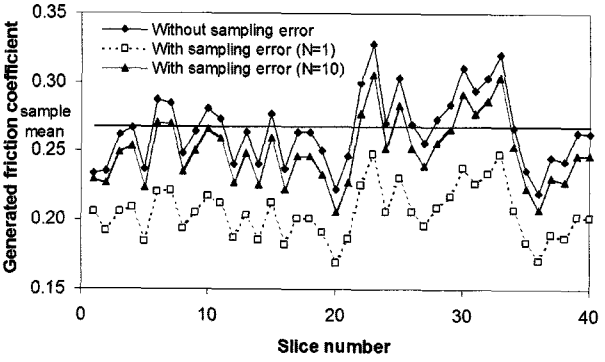

(b) with Trend Lower than Sample Mean; N: Number of Samples

Fig. 5. Samples of Generated Friction Coefficients over the 40 Slices of the Slip Surface

For the purpose of this seismic analysis, the landfill slope is assumed to be in Berkeley, California, in the seismically active San Francisco Bay Area. The major faults affecting the region are the San Andreas, Hayward, and Calaveras faults, all within 30 kilometers of the site. Based on the regional seismicity, seismic hazard analyses, using the empirical RMS attenuation relationship (Kavazanjian et al. 1985), are performed. All the major and minor faults in the vicinity of the site including background sources are considered. The computed RMS hazards are then de-aggregated into several intervals of intensity, magnitude, and distance. In order to generate RMS-compatible ground motion, we need to specify the frequency content and duration in addition to the RMS acceleration. The author adopts the stochastic ground motion parameters suggested by Wang and Kavazanjian (1987) and updated by Tung et al. (1992). Tables 2 and 3 summarize stochastic ground motion parameters used in this study. The frequency content of the ground motion is modeled by dividing the motion into three sections of equal time interval within which stationarity of the frequency content is assumed.

Another strong ground motion parameter, which is important in nonlinear deformation analyses, is duration. The hazard compatible duration can be assigned to each generated ground motion by means of de-aggregation of total hazard into appropriate intervals of earthquake magnitude and distance to site. Kim(2003) reported the

Table 2. Power spectral density parameters for rock sites (from Tung et al. 1992)

Parameter	Distribution	Segment 1		Segment 2		Segment 3	
		μ	σ	μ	σ	μ	σ
ω_g	Gamma	23.57	3.46	21.12	3.60	18.38	3.50
ζ_g	Gamma	0.352	0.360	0.394	0.380	0.417	0.162

Table 3. Parameters for modulating function (from Wang and Kavazanjian 1987)

Parameter	Distribution	μ	σ
α	Rayleigh	0.73	0.45
β	Exponential	0.22	0.18

significant duration, which is estimated using the empirical relationship proposed by Abrahamson and Silva (1996).

Figure 6 shows the geometry of the problem and the dynamic soil properties, used in the 1-D ground response analyses of the landfill slope, in which the 2-D geometry is approximated by 1-D problem. Modulus reduction and damping curves proposed by Singh and Murphy (1990), and by Schnabel (1973) are used for the waste and base rock respectively. Although shear wave velocity of the solid waste is known to increase with depth, uniform shear wave velocity is assumed so as to be consistent with the assumed homogeneous site condition. The horizontal equivalent acceleration (*HEA*) time history (or the average seismic coefficient k_{ave}) acting on the sliding mass on slope is estimated through seismic response analyses. The procedure needs the shear stress time history $\tau_h(t)$, as described by Bray and Rathje (1998). The shear stress time history at the base of potential sliding mass is evaluated with 1-D wave analyses by using SHAKE91

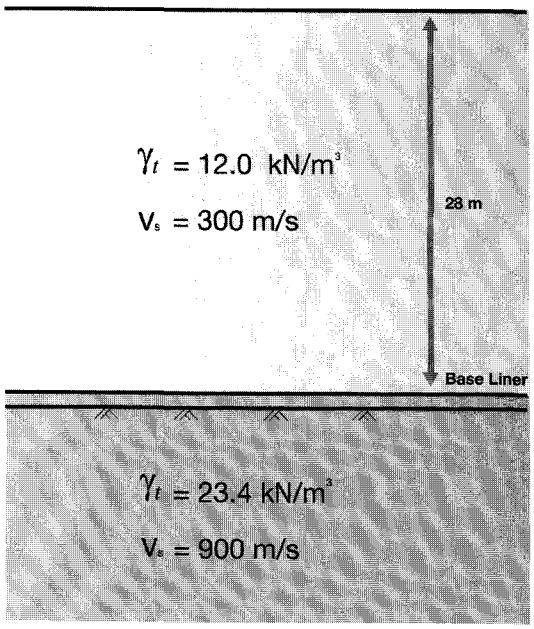

Fig. 6. Geometry of the 1-D Approximation of the Landfill and Dynamic Soil Properties

(Idriss and Sun 1992). Unlike the deformation analyses, the ground response analyses are performed by assuming that the key soil properties are deterministic, hence using mean values of the properties. This approach is adopted, since we employ the decoupled approach, in which ground response and slope deformation analyses are performed separately, by using separate numerical programs (otherwise, in a strict sense, correlations between input parameters of ground response and deformation analyses should be considered). Ideally, the ground response and deformation analyses are performed in so-called coupled mode, thus eliminating the need to provide separate sets of input parameters, as in the case of the decoupled analyses. On the other hand, the coupled analyses such as dynamic FEM are generally time-consuming, and cannot be used routinely, even in the current fast computing environment. This is even more so in inherently time-consuming probabilistic analyses, which generally involve a significant number of repeated analyses of the problem.

The slope is assumed to be able to tolerate up to 300 mm of permanent base displacement. Presently, no standard for acceptable permanent deformation has been established, but in practice it is generally assumed that maximum seismic displacements of 15-30 cm are tolerable for well-designed lined waste fills (i.e., Seed and Bonaparte 1992).

Simulation-based (Monte Carlo) reliability analyses are performed by generating a series of hazard compatible outcrop rock motions, and by using them in subsequent 1-D ground response and slope deformation analyses. The computations are carried out both for the case, where spatial variation is only considered, and the case, where uncertainty arising from sampling is also considered, in order to compare their relative significance on the risk of failure. The results are shown in Figure 7. The seismic hazards (Figure 7a) are the same for the four cases. The difference is the level of uncertainty in soil property determination. The deterministic soil properties represent the lowest level of uncertainty in the property determination, the "with sampling error added" the highest level of uncertainty, and the "spatial variation only" in between these levels. The case of deterministic mean soil

properties provides the lower bound of the risk and the mean minus standard deviation yields the upper bound.

It can be seen in Figure 7b that all three cases except the case of the mean minus standard deviation are almost identical for all RMS levels larger than 0.1 g. In other words, the risk of failure is not sensitive to the uncertainty of material properties. That is possibly due to significant spatial averaging effects and also relatively large number of samplings. It may be thus argued in this particular case that seismic uncertainty is the dominant factor in the assessment of stability of the slope, and that material uncertainty maybe neglected without significant impact on the computed reliability of the problem. The results suggest that in a highly seismically active region, characterization of earthquake hazard is the most important and that characterization of soil properties, if in a reasonable range, have a relatively small effect on the computed risk of the slope failure.

Figure 7c shows that the most probable failure event will come from the RMS hazard of 0.2-0.3 g due to their relatively high rates of occurrence and damaging effects. This information may be useful in case we need to determine earthquake scenarios that are associated with the corresponding probabilistic hazard level.

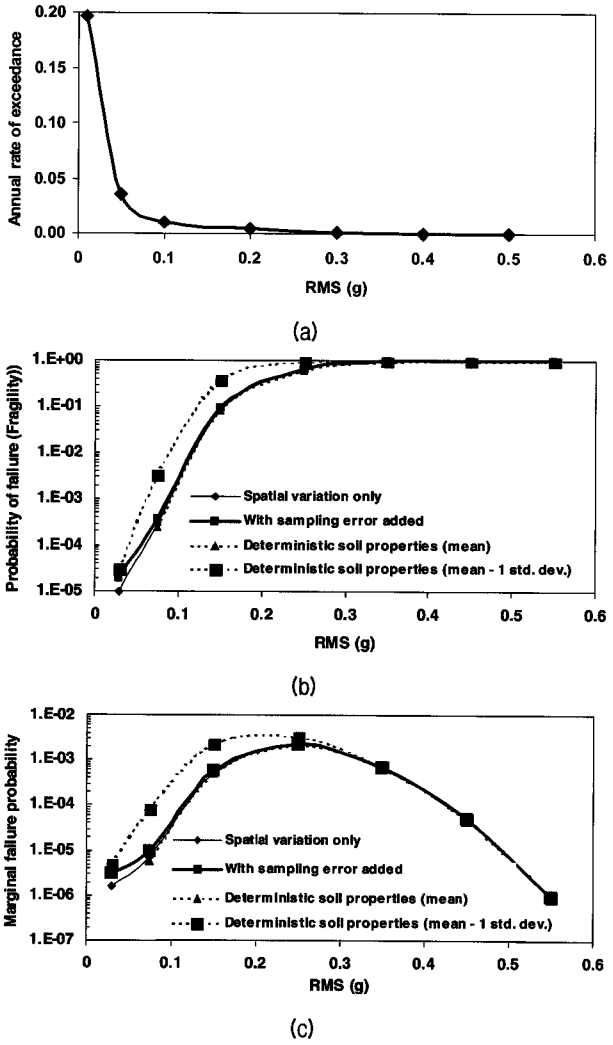

Fig. 7. (a) Annual Hazard Curve (Annual Rate of Exceeding Each Hazard Level); (b) Fragility Curve; (c) Marginal Annual Risk Curve (Annual Probability of Failure with Respect to Each Hazard Level)

4.2 Circular Slip Surface

The slope (Figure 8) reported by Kim (2003) is revisited in order to see the consistency of findings in the analysis above persists in different types of slope. The results were described by Kim (2003) and therefore, are briefly discussed here only for comparison purpose. This paper, however, reports some of findings from the follow-up study that examines the influence of scales of fluctuation in the seismic slope stability.

Three vertical borings are carried out and 10 soil samples are taken at the specific locations shown in Figure 8. Laboratory tests yield a sample mean value $\bar{c} = 45$ kN/m^2 with standard deviation $s_c = 13.5$ kN/m^2 for undrained shear strength, and $\bar{\gamma} = 18$ kN/m^3 and $s_\gamma = 0.9$ kN/m^3 for soil density. The soil deposit is modeled as a statistically homogeneous random field with two different scales of fluctuation (a measure of correlation distance) $\delta_x = 5$ m and $\delta_y = 1$ m, and $\delta_x = 25$ m and $\delta_y = 5$ m, respectively. In addition to the shear strengths it is assumed that the shear wave velocity measured at the site may be around

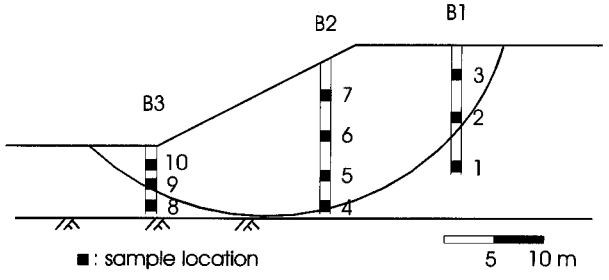

Fig. 8. Geometry and Sample Location of a Slope with a Circular Slip Surface (Kim 2003)

200 m/sec. The potential sliding mass is divided into 40 vertical soil slices of equal width, for subsequent seismic stability and deformation analyses.

The slope is also assumed to be in Berkeley. Unlike the preceding example, only the Hayward fault that is the closest major fault to the site is considered here.

The computations were carried out with the soil properties modeled with various approaches including conditional, unconditional and deterministic methods (Kim 2003). Figure 9 shows the probabilities of failure given the certain hazard levels (often called *fragility curve*), for five different characterizations of soil properties. It is interesting to observe that the differences in the probabilities of failure for the different cases are significant at the lower level of hazard (< 0.1 g) and gradually decrease with increasing hazard level, being negligible at the higher level (> 0.2 g) except for the case of the mean minus one standard deviation (i.e., conservative assessment of soil properties). For relatively small correlation lengths ($\delta_x = 5\ m$ and $\delta_y = 1\ m$), the difference between the conditional and unconditional (with sampling error) approaches is minimal. Increasing correlation ($\delta_x = 25\ m$ and $\delta_y = 5\ m$) yields a similar trend, but the risk level for the unconditional approaches becomes higher due to small variance reduction. Thus, in this particular problem, uncertainty of soil properties has a significant impact on the computed risk of slope failure at relatively low levels of seismic hazard, but it has little impact on the computed risk if the slope is exposed to relatively high levels of hazard. In this particular problem, the uncertainty of soil properties arising from the spatial variation and sampling errors does not have much impact on the reliability of the slope for the RMS hazard level higher than 0.2 ~ 0.3 g. The results are consistent with those from the previous non-circular slope case

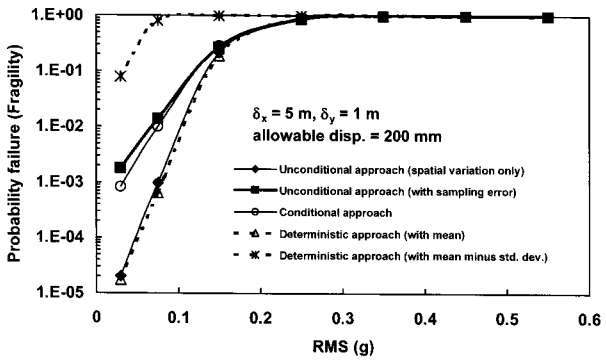

Fig. 9. Probability of Failure Given the Certain Hazard Levels (Fragility Curve)

5. Summary and Conclusions

The effects of the material and seismic load uncertainties on the performance of different types of slopes were investigated and a new reliability-based method for evaluating permanent deformations of slopes was presented. The stochastic nature of seismic loading was accounted for by generating a large series of hazard-compatible artificial motions, and by using them in subsequent response analyses. The uncertainty of material properties was also considered. The developed method can model both material and seismic hazard uncertainties at the same time unlike other previous studies.

The RMS acceleration was adopted to characterize the intensity of ground shaking. The RMS procedure proved to be useful for generation of a large number of hazard-compatible motions, unlike the conventional procedures that usually can generate only a small number of motions that match deterministic targets such as design response spectra.

It is found that for relatively small correlation lengths, the difference between the conditional and unconditional (with sampling error) approach is minimal. Increasing correlation yields a similar trend, but the risk level for the unconditional approaches becomes higher due to small variance reduction.

Two example problems show that the characterization of material properties has a considerable influence on the probability of failure for a slope that is exposed to relatively low levels of seismic hazard. On the other hand, it shows a little impact on the computed risk in case of relatively high levels of seismic hazard.

The results suggest that in a seismically active region like the Western States of USA, Taiwan and Japan, characterization of earthquake hazard is the more critical factor in the computed risk, and a moderate variability in material properties and its characterization have a

relatively small effect on the computed risk of slope failure and excessive slope deformations. On the other hand, in a seismically less active region like the Mid-Western States of USA, Britain and Korea, characterization of material properties may be equally important to that of earthquake hazard, and therefore cannot be neglected.

Acknowledgments

This research was supported for two years by the Pusan National University Research Grant. The author thanks professor Sitar of University of California at Berkeley for reviewing the manuscript.

References

1. Abrahamson, N., and Silva, W. (1996), *Empirical Ground Motion Models, Draft Report*, Brookhaven National Laboratory.
2. Abrahamson, N., and Silva, W. (1997), "Empirical Response Spectral Attenuation Relations for Shallow Crustal Earthquakes", *Seismological Research Letters*, Vol.68, No.1, pp.94-127.
3. Augello, A. J., Matasovic, N., Bray, J. D., Kavazanjian, J., E., and Seed, R. B. (1995), "Evaluation of Solid Waste Landfill Performance During the Northridge Earthquake", *Geotechnical Special Publication*, No.54, ASCE, pp.17-50.
4. Bolt, B. A. (1969), "Duration of Strong Ground Motion", *Proceedings of Fourth World Conference on Earthquake Engineering*, Santiago, Chile, pp.1304-1315.
5. Bray, J. D., and Rathje, E. M. (1998), "Earthquake-Induced Displacements of Solid-Waste Landfills", *Journal of Geotechnical and Geoenvironmental Engineering*, ASCE, Vol.124, No.3, pp.242-253.
6. Gasparini, D. A., and Vanmarcke, E. H. (1976), *Evaluation of Seismic Safety of Buildings Report No. 2: Simulated Earthquake Motions Compatible with Prescribed Response Spectra*, Publication No.R76-4, Department of Civil Engineering, Massachusetts Institute of Technology, Cambridge, Massachusetts.
7. Housner, G. W. (1952), *Intensity of Ground Motion During Strong Earthquake*, California Institute of Technology, Earthquake Research Laboratory.
8. Housner, G. W. (1975), "Measures of Severity of Earthquake Ground Shaking", *Proceedings U.S. National Conference on Earthquake Engineering*, Ann Arbor, Michigan.
9. Idriss, I. M. (1991), *Selection of Earthquake Ground Motions at Rock Sites*, Report prepared for the Structures Division, Building and Fire Research Laboratory, NIST.
10. Idriss, I. M., and Sun, J. I. (1992), *User's Manual for SHAKE91 - A Computer Program for Conducting Equivalent Linear Seismic Response Analyses for Horizontally Layered Soil Deposits*, Center for Geotechnical Modeling, Department of Civil and Environmental Engineering, University of California, Davis, California.
11. Kanai, K. (1957), "Semi-Empirical Formula for the Seismic Characteristics of the Ground", *Bulletin of the Earthquake Research Institute*, Tokyo University, Vol.35, pp.308-325.
12. Kavazanjian, J., E., Echezuria, H., and McCann, J., M. W. (1985), "RMS Acceleration Hazard for San Francisco", *Soil Dynamics and Earthquake Engineering*, Vol.4, No.3, pp.106-123.
13. Kim, J. (2003), "The Importance of Geotechnical Variability in the Analysis of Earthquake-Induced Slope Deformations", *Journal of Korean Geotechnical Society*, Vol.19, No.2, pp.123-133
14. Kim, J., Bray, J., Riemer, M. (2005), "Dynamic Properties of Geosynthetic Interfaces", *Geotechnical testing Journal*, ASTM, Vol.28, Issue 3, pp.288-296.
15. Kim, J., and Sitar, N. (2004), "Direct Estimation of Yield Acceleration in Seismic Slope Stability Analyses", *Journal of Geotechnical and Geoenvironmental Engineering*, ASCE, Vol.130, No.1, pp.111-115.
16. Liu, P. L., Lin, H. Z., and Der Kiureghian, A. (1989), *CALREL User Manual*, Report No. UCB/SEMM-89/18, Department of Civil Engineering, University of California at Berkeley, Berkeley, California.
17. Newmark, N. M. (1965), "Effects of Earthquakes on Dams and Embankments", *Geotechnique*, Vol.15, No.2, pp.139-160.
18. Pal, S. K., Rahman, M. S., and Tung, C. C. (1991), "A Probabilistic Analysis of Seismically Induced Permanent Movements in Earth Dams", *Soils and Foundations*, Vol.31, No.1, pp.47-59.
19. Rice, S. O. (1954), "Mathematical Analysis of Random Noise", *Selected Papers on Noise and Stochastic Processes*, N. Wax, ed., Dover Publications, New York, pp.133-294.
20. Rubinstein, R. Y. (1986), *Monte Carlo Optimization, Simulation and Sensitivity of Queueing Networks*, John and Wiley & Sons, New York.
21. Saragoni, G. R., and Hart, G. C. (1974), "Simulation of Artificial Earthquakes", *Earthquake Engineering and Structural Dynamics*, Vol.2, pp.249-267.
22. Schnabel, P. B. (1973), *Effects of Local Geology and Distance from Source on Earthquake Ground Motions*, Ph.D. Dissertation, University of California, Berkeley, California.
23. Seed, R. B., and Bonaparte, R. (1992), "Seismic Analysis and Design of Lined Waste Fills: Current Practice", *ASCE Special Conference on Stability and Permanent Deformation of Slopes and Embankments*, II, Reston, Va, pp.1152-1187.
24. Seed, R. B., Mitchell, J. K., and Seed, H. B. (1990), "Kettleman-Hills Waste Landfill Slope Failure. 2: Stability Analyses", *Journal of Geotechnical Engineering*, ASCE, Vol, No.4, pp.669-690.
25. Singh, S., and Murphy, B. (1990), "Evaluation of the Stability of Sanitary Landfills", *Geotechnics of Wastefills - Theory and Practice*, ASTM STP 1070, ASTM, pp.240-258.
26. Tajimi, H. (1960), "A Statistical Method of Determining the Maximum Response of a Building Structure During an Earthquake", *Proceedings of the Second World Conference on Earthquake Engineering*, Tokyo, pp.781-797.
27. Trifunac, M. D., and Brady, A. G. (1975), "A Study of the Duration of Strong Earthquake Ground Motion", *Bulletin of the Seismological Society of America*, Vol.65, pp.581-626.
28. Tung, A. T. Y., Kiremidjian, A. S., Wang, J. N., and Kavazanjian, J., E. (1992), "Statistical Parameters of AM and PSD Functions for the Generation of Site-Specific Strong Ground Motions", *Earthquake Engineering, Tenth World Conference.*

29. Wang, J. N., and Kavazanjian, J., E. (1987), *A Nonstationary Probabilistic Model for Pore Pressure Development and Site Response due to Seismic Excitation*, Report No.84, The John A. Blume Earthquake Engineering Center, Stanford University.
30. Yang, J.-N. (1973), "On the Normality and Accuracy of Simulated Random Processes", *Journal of Sound and Vibration*, Vol.3, pp.417-428.
31. Yegian, M. K., Marciano, E. A., and Ghahraman, V. G. (1991), "Earthquake-Induced Permanent Deformations - Probabilistic Approach", *Journal of Geotechnical Engineering*, ASCE, Vol.117, No.1, pp.35-50.

(received on Jan. 18, 2007, accepted on Mar. 20, 2007)